Core-shell structured nanoporous N-doped carbon decorated with embedded Co nanoparticles as bifunctional oxygen electrocatalysts for rechargeable Zn-air battery

Xiaowen Chen [a], Jingxia Gao [a], Luyuan Wang [a], Ping Zhu [a], Xinsheng Zhao [b,*],
Guoxiang Wang [c], Sa Liu [a,**]

[a] School of Chemistry and Materials Science, Jiangsu Normal University, Xuzhou, 221116, China

[b] School of Physics and Electronic Engineering, Jiangsu Normal University, Xuzhou, 221116,
China

[c] School of Light Industry & Chemical Engineering, Dalian Polytechnic University, Dalian,
116034, China

Experimental Section

Materials characterization

The morphology of the samples was characterized by Hitachi S-8010 scanning electron microscopy (SEM) and FEI Tecnai G2 F20 field emission transmission electron microscopy (TEM). X-ray diffraction (XRD) was carried out by Bruker AXS D8 ADVANCE at 40 kV with Cu Kα radiation (λ=1.5418 Å). X-ray photoelectron spectroscopy (XPS) spectra were collected on ESCALAB 250Xi. Raman spectroscopy was obtained on LabRAM HR800 under 532 nm laser excitation. The

---

* Corresponding author, xinshengzhao@jsnu.edu.cn (X. Zhao).
** Corresponding author. liusa@jsnu.edu.cn (S. Liu).

nitrogen absorption isotherm was tested with Quantachrome Autosorb IQ 2-VP instrument.

Electrochemical measurements

The electrochemical test was carried out by CHI700 electrochemical workstation at room temperature. Platinum wire was used as the electrode, and the reference electrode was Ag/AgCL electrode with 3.5 M KCl. The working electrode was prepared as follows: 5 mg of the prepared catalyst was dispersed into 0.6 mL of ethanol and 50 µL of Nafion (5 wt.%). The dispersion was homogenized by ultrasound to form an ink-like feed liquid. Then, the mixed solution of 10 µL was dripped on the pre-cleaned rotating disk electrode (RDE) or rotating-ring disk electrode (RRDE) to form a catalyst film with a load of 612 µg cm^{-2}. The working electrode with commercial Pt/C (20 wt.%) for comparison is also prepared by the same method, with a load of 100 µg cm^{-2} (*i.e.*, 20 µg$_{Pt}$ cm^{-2}) and 200 µg cm^{-2}, respectively. All the potentials in this paper were converted to the standard hydrogen electrode potential (RHE) according to $E_{RHE} = E_{measured} + E_{\emptyset Ag/AgCl}(0.207\ V\ at\ 20\ ℃) + 0.059 \times PH$.

The catalysts were electrochemically activated by cyclic voltammetry (CV) at a scan rate of 100 mV s^{-1} in N$_2$-saturated 0.1 M KOH to obtain steady curves. The ORR and OER polarization curves were obtained by linear scan voltammetry (LSV) at a scan rate of 10 mV s^{-1} and electrode rotating rate of 1600 rpm in O$_2$-saturated 0.1 M KOH between 0-1.2 V and 1.0-1.8 V, respectively.

The peroxides generated at the disk electrode during the reaction were detected by RRDE. The voltage of platinum ring was set to 1.2 V during the test. The electron transfer number (n) and the yield of hydrogen peroxide during ORR reaction were calculated by the following equation:

$$n = 4 * \frac{I_D}{I_D + I_R/N} \tag{1}$$

$$\eta_{H_2O_2} = 2 * \frac{I_R/N}{I_D + I_R/N} * 100\% \tag{2}$$

Where, I_D is the disk current, mA; I_R is the ring current, mA; N is the collection coefficient of ring disk (0.424).

The CV curves were recorded in a non-Faradic region (1.07-1.13 V) in 0.1 M KOH electrolyte at various scan rates (2, 4, 6, 8, 10 mV s^{-1}) (**Fig. S6**). Then, the capacitive current density of $\Delta j_{|ja\text{-}jc|}$ @1.10 V/2 were plotted as a function of the CV scan rate. These data are fit to a line, the slop of which is the geometric C_{dl} (mF cm^{-2}).

The stability of ORR was researched by CV test for 10000 cycles from 0.6 V to 1.2 V with a sweep rate of 200 mV s^{-1}. The durability towards OER was measured by chronopotentiometry at 10 mA cm^{-2}.

Fabrication of ZABs

For an aqueous ZAB, the anode was zinc plate with a thickness of 0.1 mm. The air electrode was fabricated as follows: a certain of the above catalyst ink was uniformly dropped on a gas diffusion layer (GDL) attached on carbon cloth (active area of 1.0 cm^{-2}), and the catalyst loading was 1.0 mg cm^{-2}. The air electrode with 1.0 mg cm^{-2} of commercial 20% Pt/C+RuO$_2$ (with a mass ratio of 1:1) was also prepared

by a similar method. 6.0 M KOH and 6.0 M KOH containg 0.2 M zinc acetate were used as electrolyte for primary and rechargeable ZABs, respectively.

The solid-state ZAB was assembled with a button structure (**Fig. S13**), following the sequence of stainless steel anode casing, zinc plate anode, gel electrolyte, catalyst-loaded GDL air-cathode (effective area: 1 cm^2, the catalyst loading: 1 mg cm^{-2}), nickel foam and stainless steel cathode casing. The preparation method of gel electrolyte was as follows: 1.0 g of polyvinyl alcohol (PVA) powder (M_w = 195000) was dissolved in 10.0 mL of deionized water under magnetic stirring for 0.5 h at 95 °C. Then 1.0 mL of 18.0 M KOH blended with 0.02 M zinc acetate was added, and the mixed electrolyte solution was kept stirring at 95 °C for 30 min until the solution became uniform. The solution was frozen at −2 °C over 12 h and then thawed at room temperature. The procedure was repeated twice to generate the PVA gel robustly.

ZABs were tested at room temperature. The discharge and charge polarization curves were obtained by LSV at a scan rate of 1.0 mV s^{-1} on a CHI 700D. The galvanostatic cycling under ambient atmosphere was carried out with LAND testing system.

Results
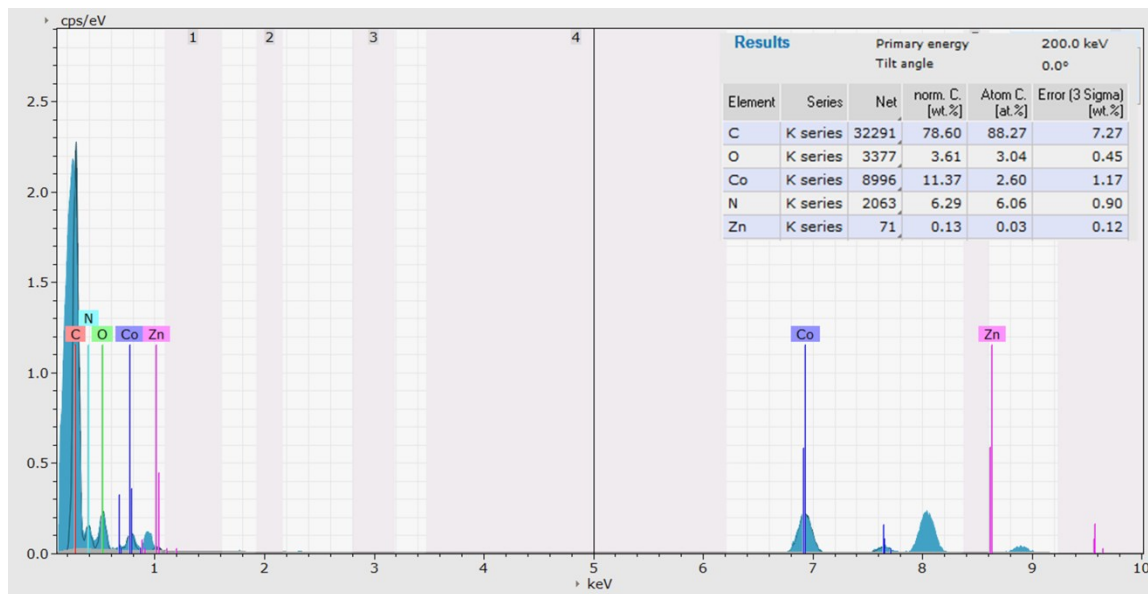
Fig. S1 EDS spectrum of PNC@CoNC.
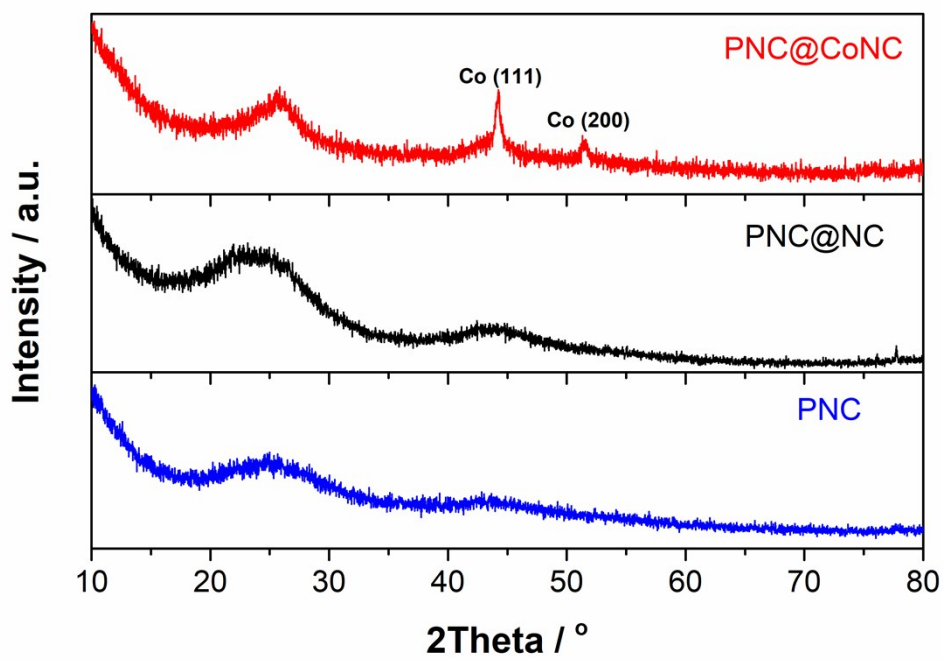
Fig. S2 XRD patterns of different catalysts.
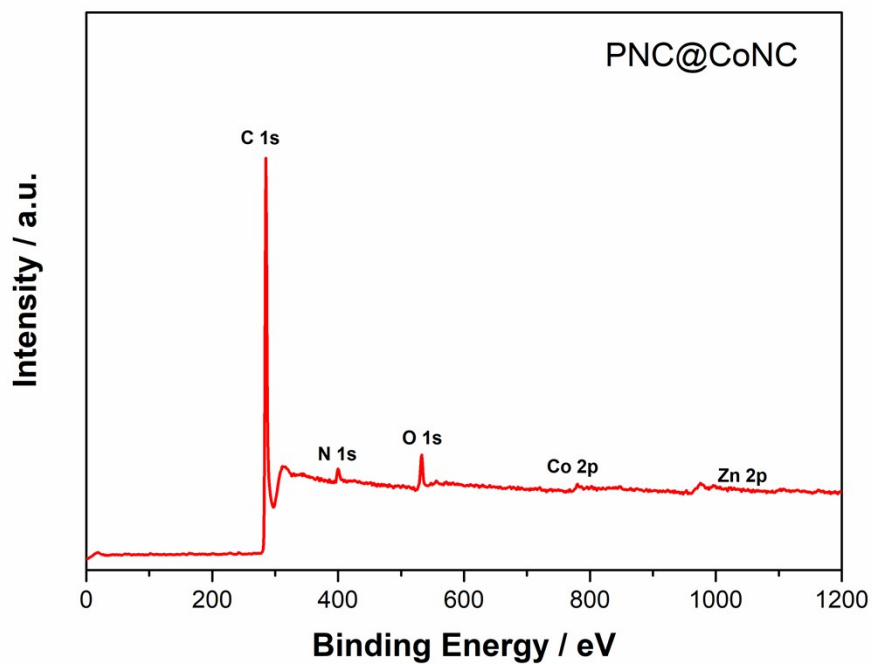
Fig. S3 XPS survey spectrum of PNC@CoNC.
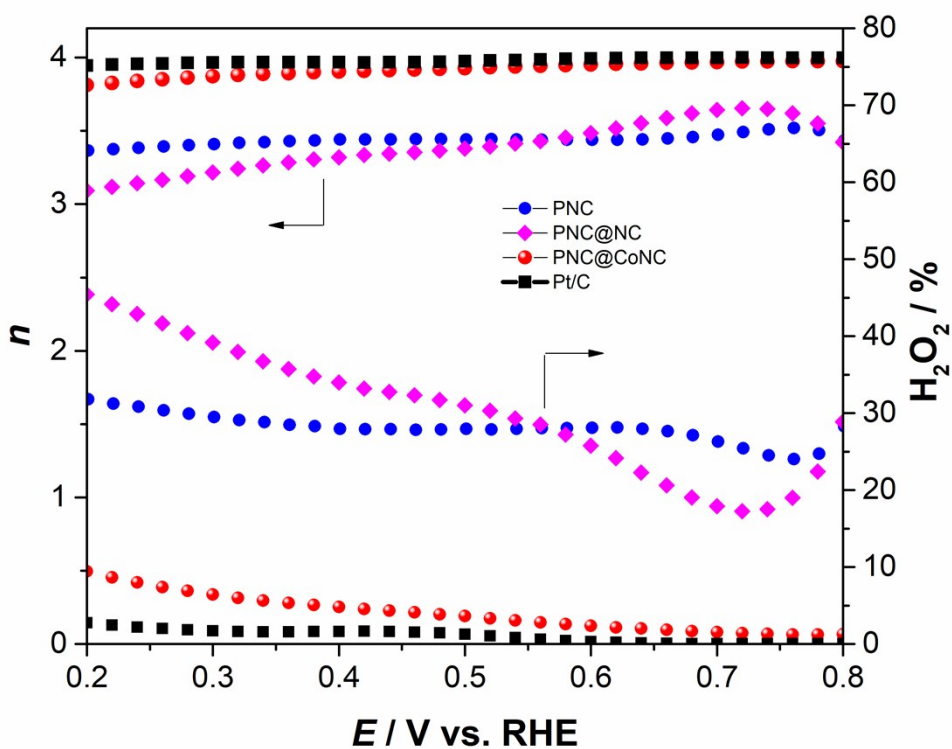
Fig. S4 The H_2O_2 yield and electron transfer number of different catalysts measured by RRDE technique.
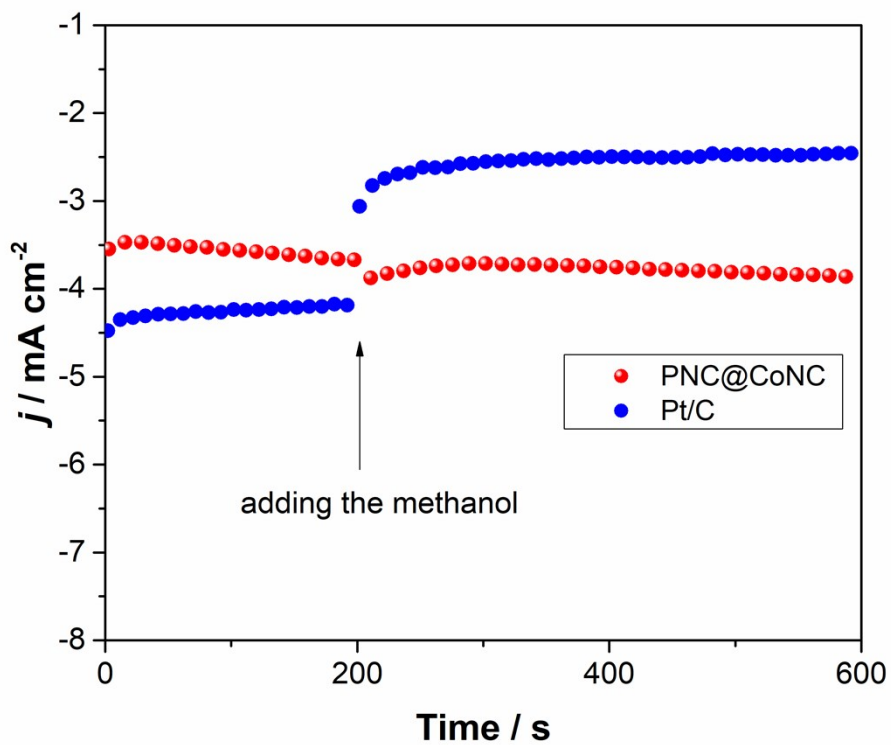
Fig. S5 The chronoamperometry curves of different catalysts in O_2-saturated 0.1 M KOH at 0.7 V *vs*. RHE.
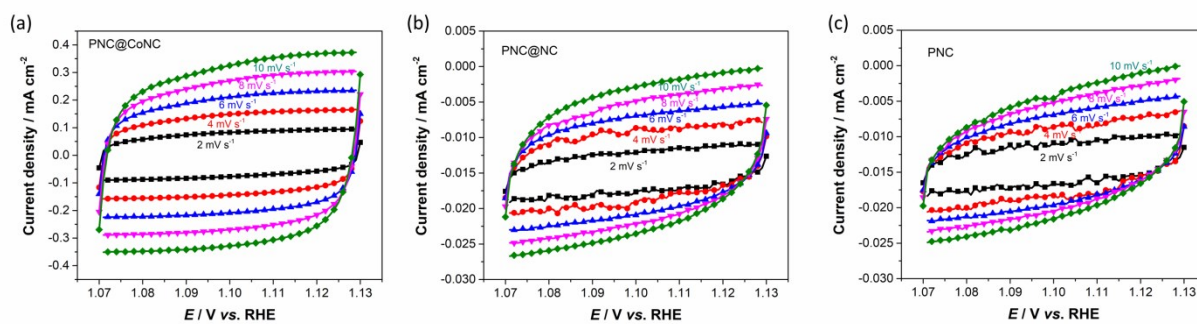
Fig. S6 CV curves of different catalysts at different scan rates in O_2-saturated 0.1 M KOH.
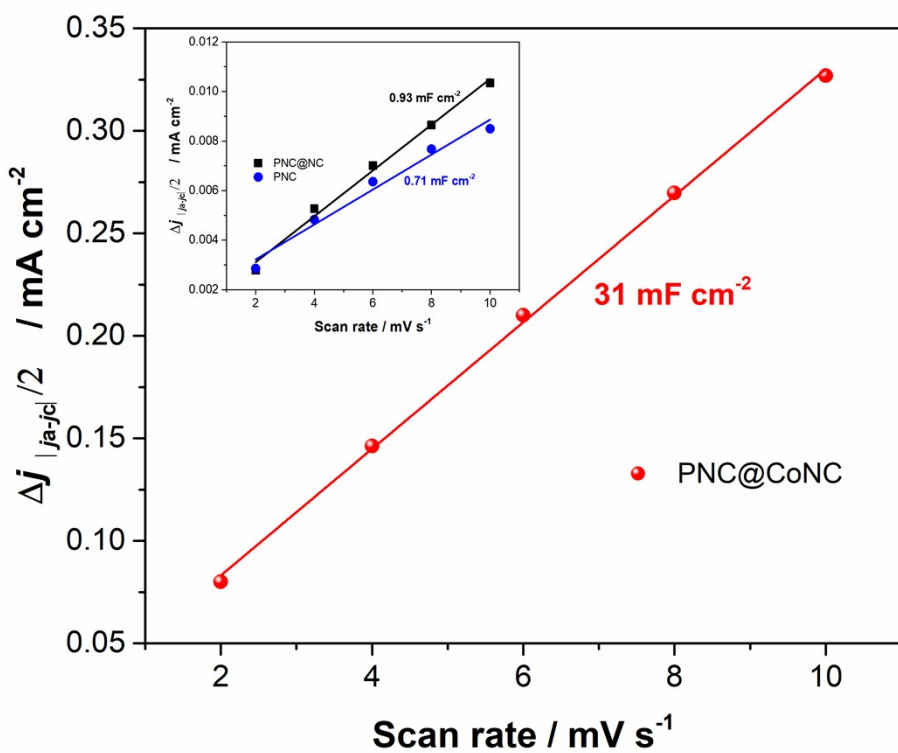
Fig. S7 Capacitive current measured at 1.10 V of as-prepare catalysts.
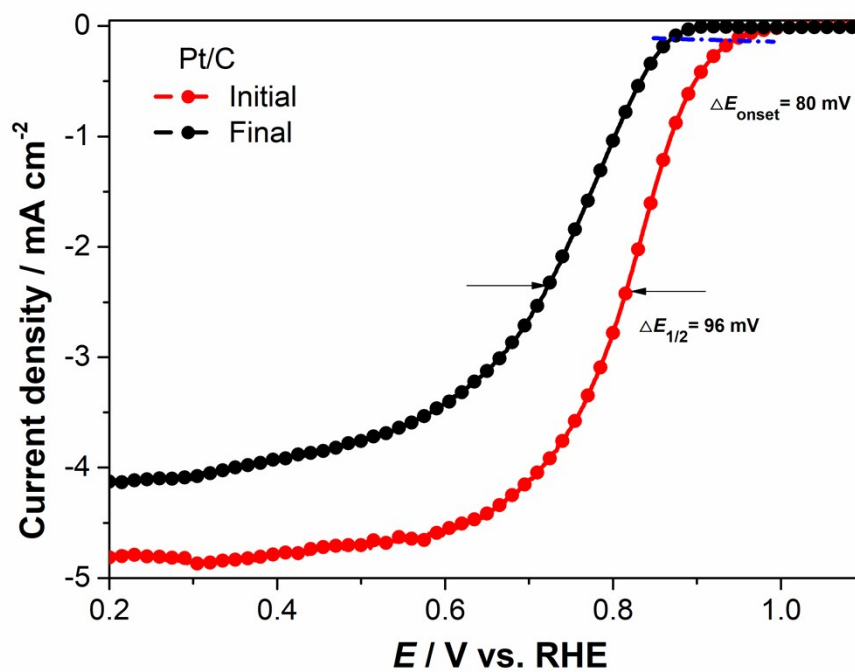
Fig. S8 The ORR polarization curves before and after 10000 CV cycles.
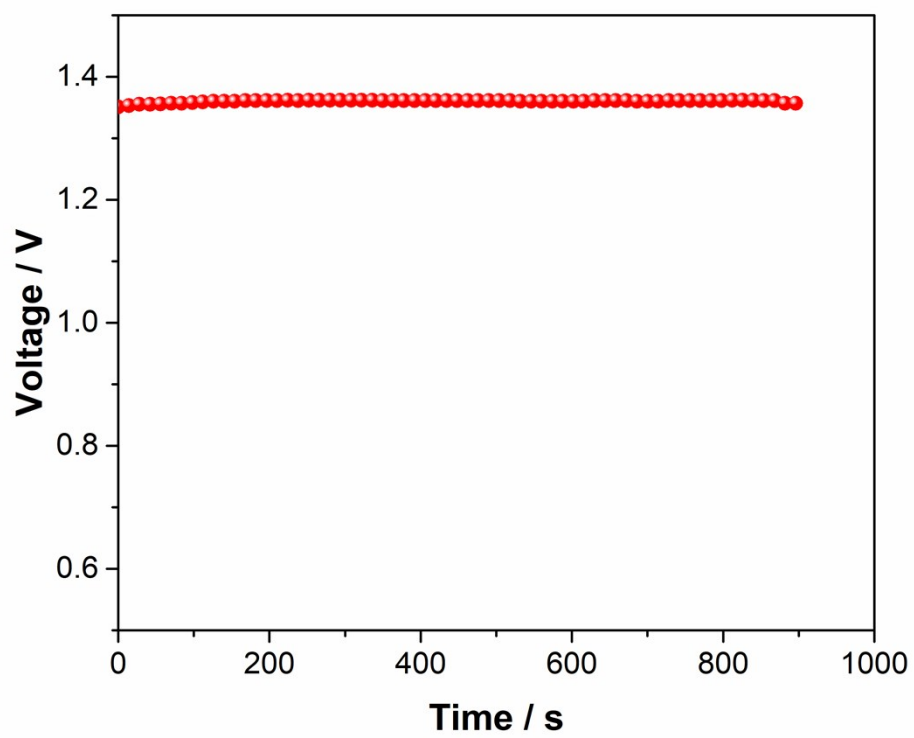
Fig. S9 The OCV curve of PNC@CoNC-based ZAB.
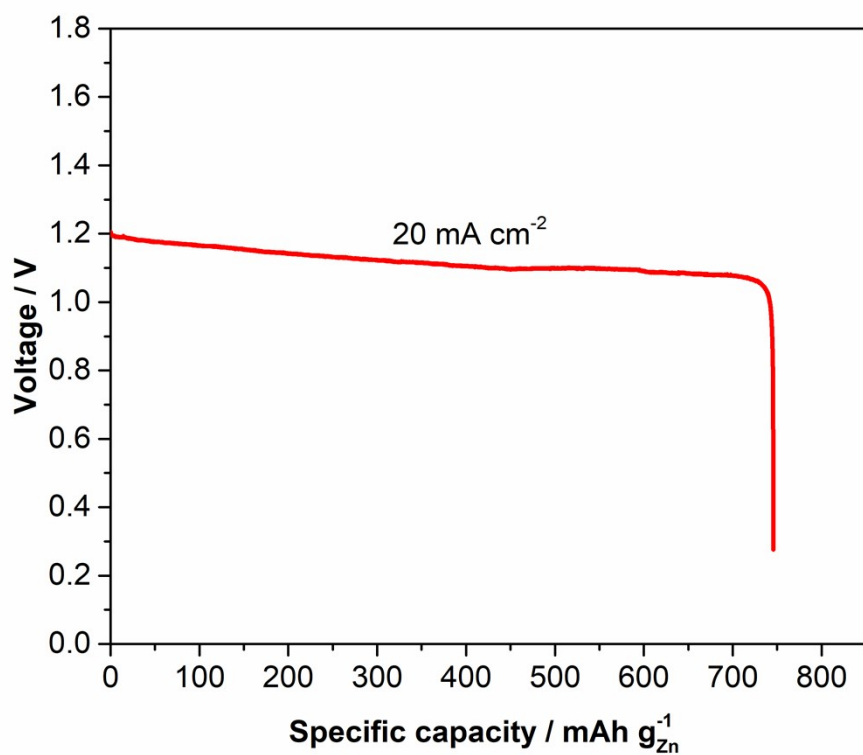
Fig. S10 The invariant current discharge curve of PNC@CoNC-based ZAB at a discharge current density of 20 mA cm^{-2}.
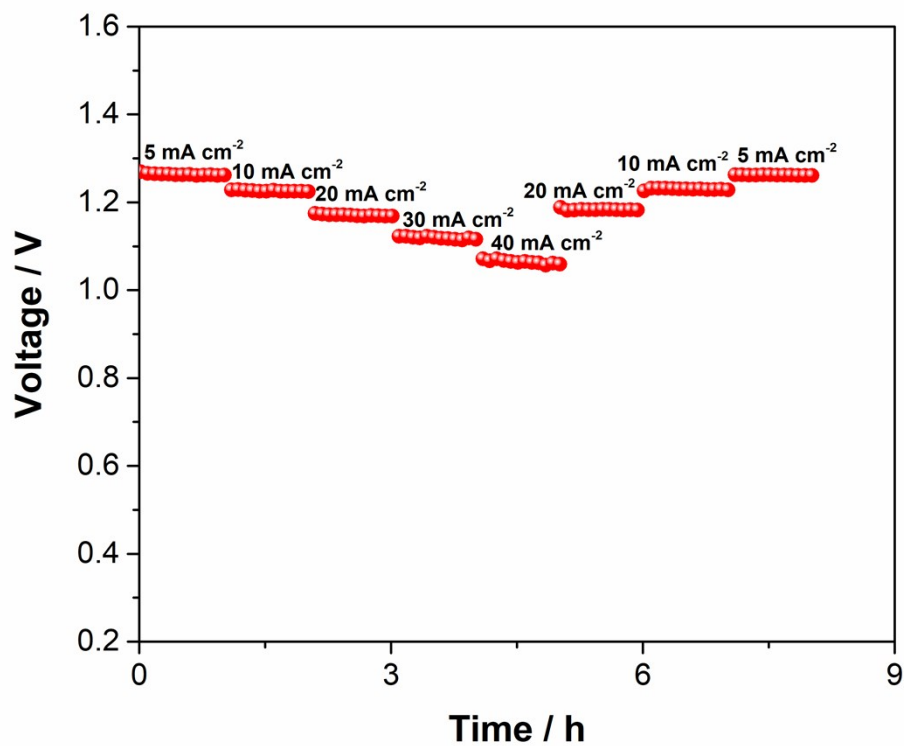
Fig. S11 The invariant current discharge curves of PNC@CoNC-based ZAB at various current densities.
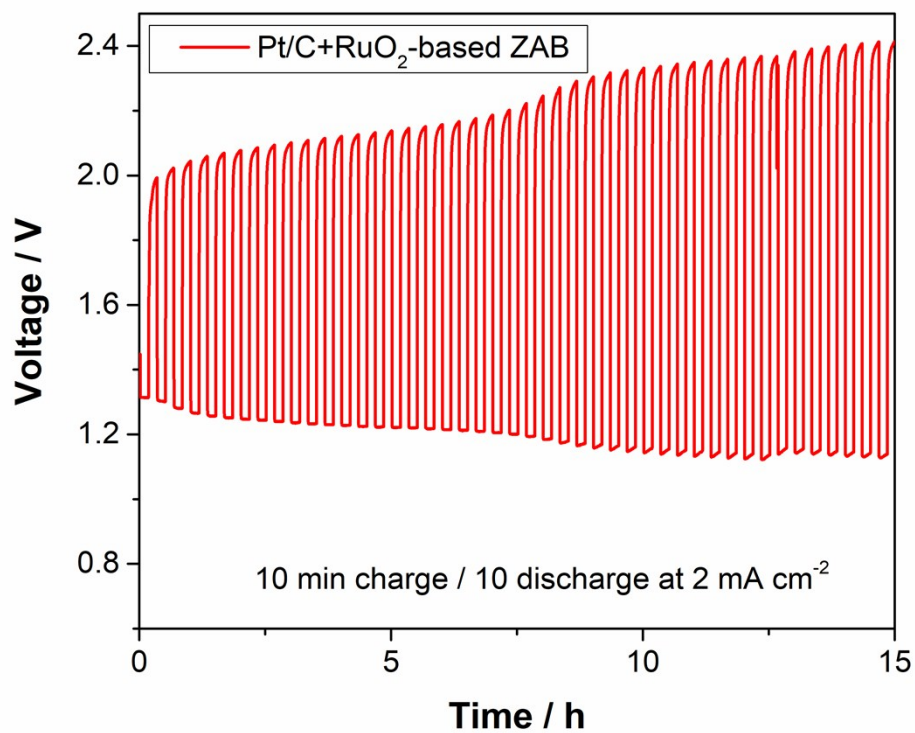
Fig. S12 Galvanostatic charge and discharge cycling curves of Pt/C+RuO$_2$-based aqueous ZAB.
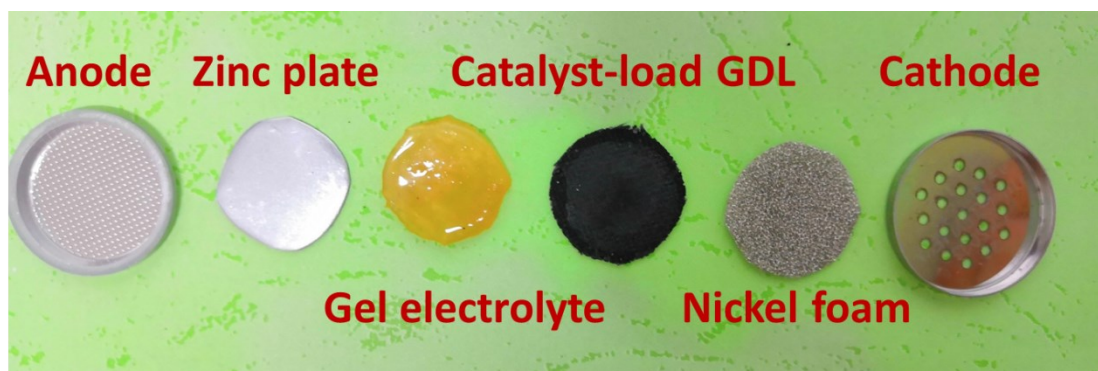
Fig. S13 Digital photo of relevant components of button ZAB.

Table S1 The ORR and OER performances of as-reported Co-based catalysts in 0.1

M KOH electrolyte.

Sample	$E_{1/2}$ (V)	E_{10} (V)	ΔE (V)	Ref.
PNC@CoNC	0.81	1.72	0.91	This work
Fe/Co-CNTs-800	0.783	1.681	0.898	[1]
Co@Co$_3$O$_4$/NC-1	0.80	1.65	0.85	[2]
Co-NC 750	0.81	1.83	1.02	[3]
Co$_3$O$_4$/N-rGO	0.79	1.72	0.93	[4]
Co-N@HCS	0.864	1.72	0.856	[5]
Co$_3$O$_4$/NPGC	0.842	1.68	0.838	[6]
NiCo$_2$S$_4$@N/S-rGO	0.76	1.7	0.94	[7]
Co/CoO$_x$@NC-CNTs	0.836	1.62	0.784	[8]
CoP–DC	0.81	1.55	0.74	[9]
Co$_{0.5}$Mn$_{0.5}$WO$_4$	0.73	1.63	0.9	[10]

Reference

[1] Y.-M. Zhao, F.-F. Wang, P.-J. Wei, G.-Q. Yu, S.-C. Cui, J.-G. Liu, Cobalt and Iron Oxides Co-supported on Carbon Nanotubes as an Efficient Bifunctional Catalyst for Enhanced Electrocatalytic Activity in Oxygen Reduction and Oxygen Evolution Reactions, ChemistrySelect, 3 (2018) 12266-12272.

[2] A. Aijaz, J. Masa, C. Rosler, W. Xia, P. Weide, A.J. Botz, R.A. Fischer, W. Schuhmann, M. Muhler, Co@Co3O4 Encapsulated in Carbon Nanotube-Grafted Nitrogen-Doped Carbon Polyhedra as an Advanced Bifunctional Oxygen Electrode, Angew Chem Int Ed Engl, 55 (2016) 4087-4091.

[3] Q. Wang, W.H. Hu, Y.M. Huang, One-Pot Synthesis of Co/Co3O4/Co(OH)2/N-Doped Mesoporous Carbon for Both Oxygen Reduction Reactions and Oxygen Evolution Reactions, ChemistrySelect, 2 (2017) 3191-3199.

[4] Y. Li, C. Zhong, J. Liu, X. Zeng, S. Qu, X. Han, Y. Deng, W. Hu, J. Lu, Atomically Thin Mesoporous Co3 O4 Layers Strongly Coupled with N-rGO Nanosheets as High-Performance Bifunctional Catalysts for 1D Knittable Zinc-Air Batteries, Adv Mater, (2017) 1703657.

[5] S. Cai, Z. Meng, H. Tang, Y. Wang, P. Tsiakaras, 3D Co-N-doped hollow carbon spheres as excellent bifunctional electrocatalysts for oxygen reduction reaction and oxygen evolution reaction, Applied Catalysis B: Environmental, 217 (2017) 477-484.

[6] G. Li, X. Wang, J. Fu, J. Li, M.G. Park, Y. Zhang, G. Lui, Z. Chen, Pomegranate-Inspired Design of Highly Active and Durable Bifunctional Electrocatalysts for Rechargeable Metal-Air Batteries, Angew Chem Int Ed Engl, 55 (2016) 4977-4982.

[7] Q. Liu, J. Jin, J. Zhang, NiCo2S4@graphene as a bifunctional electrocatalyst for oxygen reduction and evolution reactions, ACS Appl Mater Interfaces, 5 (2013) 5002-5008.

[8] S. Liu, X. Chen, S. Wang, Z. Yang, J. Gao, P. Zhu, X. Zhao, G. Wang, 3D CNTs-threaded N-doped hierarchical porous carbon hybrid with embedded Co/CoO nanoparticles as efficient bifunctional catalysts for oxygen electrode reactions, Electrochimica Acta, 292 (2018) 707-717.

[9] Y. Lin, L. Yang, Y. Zhang, H. Jiang, Z. Xiao, C. Wu, G. Zhang, J. Jiang, L. Song, Defective Carbon-CoP

Nanoparticles Hybrids with Interfacial Charges Polarization for Efficient Bifunctional Oxygen Electrocatalysis, Advanced Energy Materials, 8 (2018) 1703623.

[10] G. Karkera, T. Sarkar, M.D. Bharadwaj, A.S. Prakash, Design and Development of Efficient Bifunctional Catalysts by Tuning the Electronic Properties of Cobalt–Manganese Tungstate for Oxygen Reduction and Evolution Reactions, ChemCatChem, 9 (2017) 3681-3690.